

Ingvar Andersson
Debra M. Ikeda
Sophia Zackrisson
Mark Ruschin
Tony Svahn
Pontus Timberg
Anders Tingberg

Breast tomosynthesis and digital mammography: a comparison of breast cancer visibility and BIRADS classification in a population of cancers with subtle mammographic findings

Received: 5 February 2008
Accepted: 24 May 2008
Published online: 19 July 2008
© European Society of Radiology 2008

M. Ruschin
Department of Radiation Physics,
University Health Network/Princess
Margaret Hospital,
Toronto, ON, Canada

I. Andersson (✉) · S. Zackrisson
Diagnostic Centre of Imaging and
Functional Medicine, Malmö
University Hospital,
SE-205 02 Malmö, Sweden
e-mail: ingvar.andersson@med.lu.se
Tel.: +46-40-338865

D. M. Ikeda
Department of Radiology, Stanford
University, Stanford Advanced
Medicine Center,
Stanford, CA, USA

M. Ruschin · T. Svahn · P. Timberg ·
A. Tingberg
Department of Medical Radiation
Physics, Lund University, Malmö
University Hospital,
Malmö, Sweden

Abstract The main purpose was to compare breast cancer visibility in one-view breast tomosynthesis (BT) to cancer visibility in one- or two-view digital mammography (DM). Thirty-six patients were selected on the basis of subtle signs of breast cancer on DM. One-view BT was performed with the same compression angle as the DM image in which the finding was least/not visible. On BT, 25 projections images were acquired over an angular range of 50 degrees, with double the dose of one-view DM. Two expert breast imagers classified one-

and two-view DM, and BT findings for cancer visibility and BIRADS cancer probability in a non-blinded consensus study. Forty breast cancers were found in 37 breasts. The cancers were rated more visible on BT compared to one-view and two-view DM in 22 and 11 cases, respectively, ($p < 0.01$ for both comparisons). Comparing one-view DM to one-view BT, 21 patients were upgraded on BIRADS classification ($p < 0.01$). Comparing two-view DM to one-view BT, 12 patients were upgraded on BIRADS classification ($p < 0.01$). The results indicate that the cancer visibility on BT is superior to DM, which suggests that BT may have a higher sensitivity for breast cancer detection.

Keywords Breast · Tomosynthesis · Breast cancer

Introduction

It has been reported that 15–30% of detectable cancers in screening programmes are not detected by screen-film mammography (SFM) [1–3]. In clinical series of patients, the sensitivity of SFM for breast cancer has been reported to be 80–90%, but has been reported as low as 48% in extremely dense breasts [4]. Factors implicated in missing cancers include the technique sensitivity, distracting lesions, the tumour growth rate, the tumour growth pattern and the background upon which the tumour is displayed [5, 6].

The background on the mammogram consists of normal dense breast structures superimposed onto a two-dimensional

(2D) plane, comprising a so-called “anatomic background”. This may hamper cancer detection on conventional SFM and has been shown to play a larger role than quantum noise in the non-detection of certain lesion types and sizes [7–9]. Another factor influencing cancer visibility is the tumour growth pattern. For example, diffusely infiltrating invasive lobular carcinomas, which may not produce a mass, are often difficult to detect on mammography [10].

The introduction of digital mammography (DM) was expected to improve mammographic sensitivity for breast cancer detection. In randomised trials comparing SFM with DM, the sensitivity of mammography for cancer detection was equal or increased in DM, although the difference was

statistically significant in only one of the studies [11–14]. It could be hypothesized that the anatomic background, rather than the detector, is the limiting factor in cancer detection. If such were the case, a tomographic technique like breast tomosynthesis (BT) that reduces the obscuring effect of overlying and underlying breast tissues should improve sensitivity compared to DM [15, 16]. Even though at least some studies suggest that this might be the case [9, 17–20], these results have been mostly based on phantom studies and limited clinical data. Two recent studies showed improved specificity of BT compared with SFM [21, 22].

In the current study, our hypothesis was that the anatomic noise is a limiting factor in 2D mammography that is substantially reduced in BT. This should be most obvious in cases with subtle findings on 2D mammography. Thus, the primary objective of this study was to compare a clinical series of digital mammograms with subtle findings with BT in the same view. This was tested in a retrospective non-blinded consensus study involving two expert mammography radiologists.

Materials and methods

Patient population

The study protocol was approved by the institutional hospital committee on research and radiation safety, as well as by the Ethical Committee. All patients provided informed consent. Patients were selected from among two groups during a 12-month period (1 July 2006 to 30 June 2007):

- (1) Those from the diagnostic digital mammographic clinical population in which patients presented for evaluation of a lump or other symptom. A total of 3,251 mammographic examinations were performed in this group, among which 271 (8.3%) new cases of breast cancer were diagnosed.
- (2) Those recalled for workup from a population-based, city-wide digital mammography screening programme. During the actual period, a total of 14,345 women were screened, 493 women (3.4%) were recalled, and 78 women (0.5%) were diagnosed with breast cancer.

We included only women with subtle but suspicious findings selected from screening DM or symptomatic women with subtle or negative findings on DM but suspicious lesions on ultrasonography (US). Signs of malignancy were those generally accepted, such as mass, especially if spiculated or with irregular borders, architectural distortion, or clustered calcifications. When these signs were questionably visible, they were considered subtle; when none of the signs could be seen, the mammogram was classified as negative for malignancy. Also, on US the generally accepted signs of malignancy

were used in the analysis of US findings. One radiologist (IA) reviewed DM screening and/or diagnostic images to determine in which view—craniocaudal (CC) or mediolateral oblique (MLO)—that the DM finding was least visible or not visible at all. In patients with a suspicious lesion on US only, BT was performed in the MLO view; otherwise, BT was performed in the same orientation as the least-visible DM image. BT examinations were performed immediately following diagnostic DM/US examinations, followed by needle biopsy. All breast cancer diagnoses were verified by surgery, except for one stage IV breast cancer that was verified by core biopsy only.

Image acquisition

DM was performed on dedicated digital units (Mammomat Novation^{DR}, Siemens, Erlangen, Germany). BT was performed on a prototype unit adapted from the Mammomat Novation^{DR} (Siemens, Erlangen, Germany). The BT prototype contains a different amorphous selenium detector than the DM unit. In full-resolution mode, its detector pixel size is 85 $\mu\text{m} \times 85 \mu\text{m}$ and has properties that have been described earlier [23].

The BT images were acquired using the same tube voltage and the same anode/filter (W/Rh) combination as used for the DM images and as determined by the automatic exposure control device of the DM unit. The mean absorbed dose for DM of a standard breast [24] was 0.8 mGy. The tube loading used for the entire BT examination was twice that of a single DM image. Twenty-five projection images were acquired over an angular range of approximately 50 degrees. The detector was operated in full resolution mode, thus yielding a data acquisition time of 20 s per breast. Image reconstruction was performed by filtered backprojection [25, 26].

US was performed on a dedicated unit (Acuson Sequoia, Siemens, Erlangen, Germany) by physicians.

Viewing conditions and classification of imaging findings

DM, BT, and US examinations were reviewed on an investigational prototype version of a DM Mammo Report workstation (Siemens, Erlangen, Germany) by two expert breast-imaging radiologists in a consensus reading (IA and DMI). Comparison of clinical findings, images, and the pathology reports was done in a conjoined session by two radiologists (IA, DMI) to ensure that the imaging findings correlated to the cancer. Readings were done on two 5-mega-pixel flat-panel Dome C5i monitors (Planar Systems Inc., Beaverton, OR). The monitors were calibrated to the DICOM Grayscale Standard Display function [27]. DM, US, and BT images were available on the workstation.

There was an option of scrolling as well as zooming and altering the window level of the images.

Imaging findings and suspicion for cancer were classified on the single-view DM in which BT was performed, the two-view (CC and MLO) DM, on BT, and on US. Tumour appearances of masses, calcifications, masses plus calcifications, architectural distortions, asymmetries, or combinations of these were recorded. The visibility of the findings was classified as “not visible”, “questionably visible”, “visible”, or “clearly visible”. Finally BIRADS assessments for probability of cancer using a 1–5 classification (BIRADS) were recorded. There was only one BIRADS classification per BT examination, as only one view was acquired. For the case of two-view DM and two-view DM+US, the highest rating was always taken and used in the analysis.

Statistical analysis of BIRADS and visibility classifications

A non-parametric rank-invariant method was used to evaluate the differences in measured classification data for statistical significance [28]. The BIRADS and visibility classification scales were treated as ordinal, and no assumptions were made about their numerical distribution. A receiver-operating characteristics (ROC) type curve was generated for each technique comparison using ROCKIT (version 0.9.1 BETA) [29]. Each resulting area-under-the-curve (AUC) was reported together with a 95% confidence interval (CI₉₅). If 0.5 (i.e. the null hypothesis) was not included within the CI₉₅, then the differences between the two techniques were statistically significant at the 5% level. Additionally, a two-sided Z-test p-value for the risk of falsely rejecting the null hypothesis was determined for each comparison, assuming AUC values were normally distributed.

Classification of breast density and anatomic background

Two radiologists rated each breast for density by BIRADS categories: (1): fatty or <25% dense; (2): scattered fibroglandular densities or 25–50% dense; (3): heterogeneously dense or 50–75% dense; (4): dense or >75% dense. To further estimate the amount of obscuring dense tissue, breast tissue density 10 mm immediately around the lesion in the DM image was rated. Similarly, density on the tomographic slice showing the breast cancer in focus was rated, as was a 10-mm area around the tumour in order to determine if it corresponded with DM.

Results

The study population comprised 36 women with a combined 40 breast cancers. The women were at an

average age of 59 years old (range 34–84 years old). Eighteen women (50%, 18/36) were selected from screening, and 18 (50%, 18/36) were selected from a clinical series. Seventeen patients presented with a palpable mass or thickening and one had skin retraction. The screening sample represented 23% (18/78) and the clinical sample 7% (18/271) of the total number of cancer cases detected during the actual period of time.

Cancer pathology and radiographic cancer appearance

Out of all 40 breast cancers, 20 (50%) were invasive ductal cancers (IDC), 10 (25%) invasive lobular cancers (ILC), 5 (12.5%) IDC with ductal carcinoma in situ (DCIS), 3 (7.5%) tubular cancers, one associated with DCIS, 1 (2.5%) DCIS alone, and 1 (2.5%) intracystic papillary carcinoma. The median tumour size was 11 mm (range 5–50 mm). In Table 1 the radiographic appearance is given by modality and in relation to pathology. In three cases appearing as architectural distortion only on two-view DM, a central mass could be identified at BT, the lesions thus appearing as spiculated cancers. Two were IDC and one ILC. Three cases not seen at two-view DM were seen as spiculated masses, two representing IDC and one ILC. BT displayed masses in two cases where only calcifications were seen on two-view DM, one representing IDC, the other a tumour-forming DCIS.

BIRADS classifications for breast density on DM and BT

In 24 of 36 breasts (one patient not eligible due to juxtathoracic lesion), DM was classified as mostly dense (BIRADS 3 or 4) and less dense in the remaining 12 breasts (BIRADS 1 and 2).

The 1 cm of tissue density around the tumour on DM was the same as the overall BIRADS rating in 28 cases, decreased in 9 cases, and increased in 2 cases. On BT, the density 1 cm around the tumour stayed the same as the DM 1 cm tissue rating, except in seven cases it decreased by one BIRADS category (N=4) or by two BIRADS categories (N=3).

Cancer visibility

Cancer visibility was ranked higher for BT than for single-view DM in 22 (55%, 22/40) of the 40 cancers (Table 2, Figs. 1, 2). Thirteen of the remaining 18 cancers (32.5%, 13/40 cases) were equally visible/clearly visible on single-view DM and BT. One case was ranked higher on DM than BT; this was a spiculated cancer in a juxtathoracic location and not included in the BT field of view. The remaining four (10%, 4/40) cancers were not visible on either single-

Table 1 Forty breast cancers by appearance on one-view, two-view digital mammography (DM) or breast tomosynthesis (BT) with pathology^a

	Spiculated mass	Round mass	Calcification	Mass/calcifications	Distortion	Other	Not seen present on other view	Not seen	Total
One-view DM	7	2	5	7	7	1	4 ^b	7 ^{b,c}	40
	5 IDC	1 Intracystic mass	1 IDC	3 IDC	5 IDC	Obscured mass (ILC)	1 IDC	5 IDC	
	2 ILC	1 IDC	2 IDC/DCIS 1 DCIS 1 ILC	2 IDC/DCIS 1 ILC 1 Tubular/DCIS	1 Tubular 1 ILC		2 ILC 1 Tubular/DCIS	2 ILC	
Two-view DM	11	2	5	8	6	1		7 ^{b,c}	40
	7 IDC	1 IDC	2 IDC/DCIS	3 IDC/DCIS	3 IDC	Asymmetry (IDC)		5 IDC	
	4 ILC	1 Intracystic DCIS	1 DCIS 1 ILC	3 IDC 1 ILC 1 Tubular/DCIS	2 ILC 1 Tubular			2 ILC	
BT	16	3	4	8	4			5 ^d	40
	11 IDC	1 IDC	3 IDC/DCIS	5 IDC	1 IDC,			2 ILC	
	5 ILC	1 DCIS/Tubular 1 Intrahepatic papillary DCIS	1 ILC	1 DCIS 1 ILC 1 Tubular/DCIS	1 IDC/DCIS 1 ILC 1 Tubular			3 IDC	

^aIDC=invasive ductal carcinoma, ILC=invasive lobular carcinoma, DCIS=ductal carcinoma in situ

^bTwo spiculated masses, one distortion, one asymmetry seen on one-view only

^cFour seen by ultrasound only, two seen by BT only, one seen by ultrasound and BT

^dIncludes one spiculated mass seen on DM not included in BT field of view

view DM or BT (Fig. 3). These last four cancers were also not visible in the second DM view; all were embedded in dense tissue, and each was visible on US as a suspicious mass. The difference in visibility between the two techniques was statistically significant ($p < 0.01$).

On comparison with two-view DM, cancer visibility on BT was ranked higher than DM for 11 (27.5%, 11/40) of the

40 cancers (Table 3). The difference in visibility between the two techniques was statistically significant ($p < 0.01$).

BIRADS classifications for cancer suspicion on DM, BT, and US

Twenty-one patients were upgraded on BIRADS classification from the one-view DM compared to BT: 11 were upgraded from BIRADS 1–2 to 3–5 and 10 were upgraded from 3 to 4–5 (Table 4). The AUC for one-view BT versus one-view DM was 0.8079 [$CI_{95} = (0.6750, 0.9009)$, $p < 0.01$].

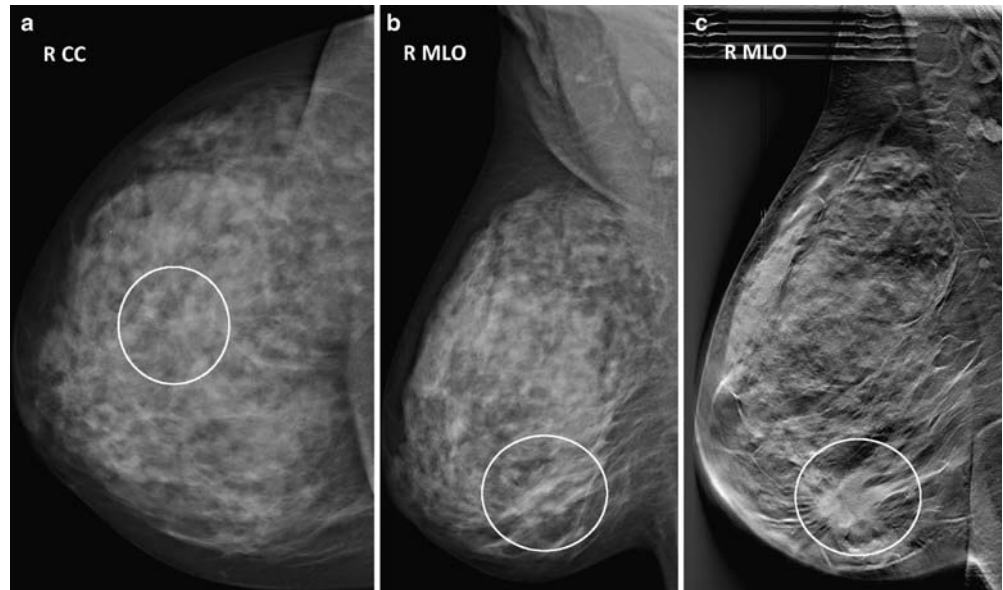
Twelve patients were upgraded on BIRADS classification from the two-view DM compared to BT: four were upgraded from BIRADS 1–2 to 3–5, and eight were upgraded from 3 to 4–5 (Table 5). The AUC for one-view BT versus two-view DM was 0.6851 [$CI_{95} = (0.5481, 0.8004)$, $p < 0.01$].

All cancers detected by US were rated as BIRADS 4 or 5. US did not detect five cancers that were later detected by BT, including two spiculated tumours later discovered in breasts containing another cancer (the breast was previously scanned by targeted US), one small mass in a fatty

Table 2 Visibility of 40 breast cancers in one-view digital mammography (DM) and one-view breast tomosynthesis (BT)

One-view DM	One-view BT	N
Not visible	Not visible	4
Not visible	Questionably visible	1
Not visible	Visible/clearly visible	6
Questionably visible	Visible/clearly visible	15
Visible/clearly visible	Visible/clearly visible	13
Clearly visible	Not visible/not included	1
Total		40

Fig. 1 Patient with a 2.8-cm, grade 3, invasive ductal carcinoma in the right breast imaged with BT and DM. (a) The CC DM view shows a slight distortion in the mid-right breast (circle). (b) The MLO DM view shows dense breast tissue with subtle distortion in the lower breast where the patient felt a mass (circle). (c) The MLO BT view shows a spiculated mass in the lower breast, much more evident than the corresponding DM image shown in (b)



breast, one cluster of suspicious calcifications, and one small distortion. One of the spiculated tumours not detected by DM or US but seen on BT was diagnosed as a grade 1, 9-mm invasive lobular carcinoma (Fig. 4). US detected five cancers undetected by BT, including four round or oval palpable cancers in dense breasts, and one spiculated tumour not included in the BT field of view.

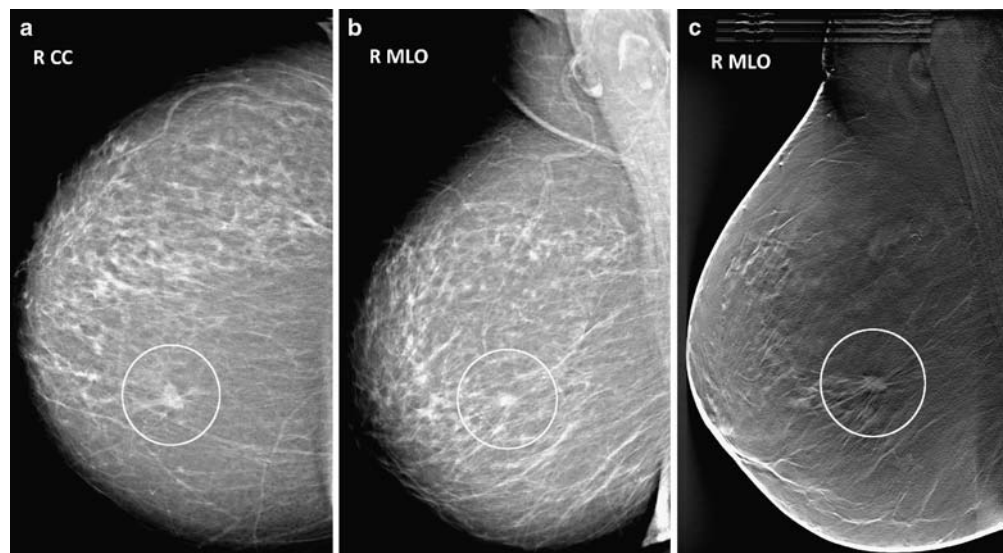
When using the combined BIRADS classifications for both the two-view DM and US as compared to BT, BIRADS suspicion for cancer was upgraded for two cancers undetected by either DM or US. On BT five BIRADS 4 lesions were downgraded to BIRADS 1, which were seen by US only (four cases) or not included in the field of view. BT downgraded two other cancers rated as BIRADS 4 by DM/US, specifically, a benign-appearing

round intracystic cancer and a cancer appearing as multiple benign-appearing nodules were rated as BIRADS 2 and 3 by BT, respectively. Two-view DM had similarly downgraded the US BIRADS 4 classification in these two cases. The BIRADS AUC for one-view BT versus two-view DM +US was 0.4040 [CI₉₅=(0.27222 0.5479), $p < 0.09$].

Discussion

The objective of this study was to compare a series of digital mammograms with subtle findings with BT. This was tested in a non-blinded consensus study. The lesions were better visualized on BT and could be classified more accurately according to BIRADS classification.

Fig. 2 Patient with a 10-mm, grade 1, invasive ductal carcinoma in a moderately dense breast imaged with BT and DM. (a) The CC DM view shows a slightly spiculated, centrally located mass (circle). (b) The MLO DM view shows a non-specific density (circle). (c) The MLO BT view clearly shows a spiculated mass (circle)



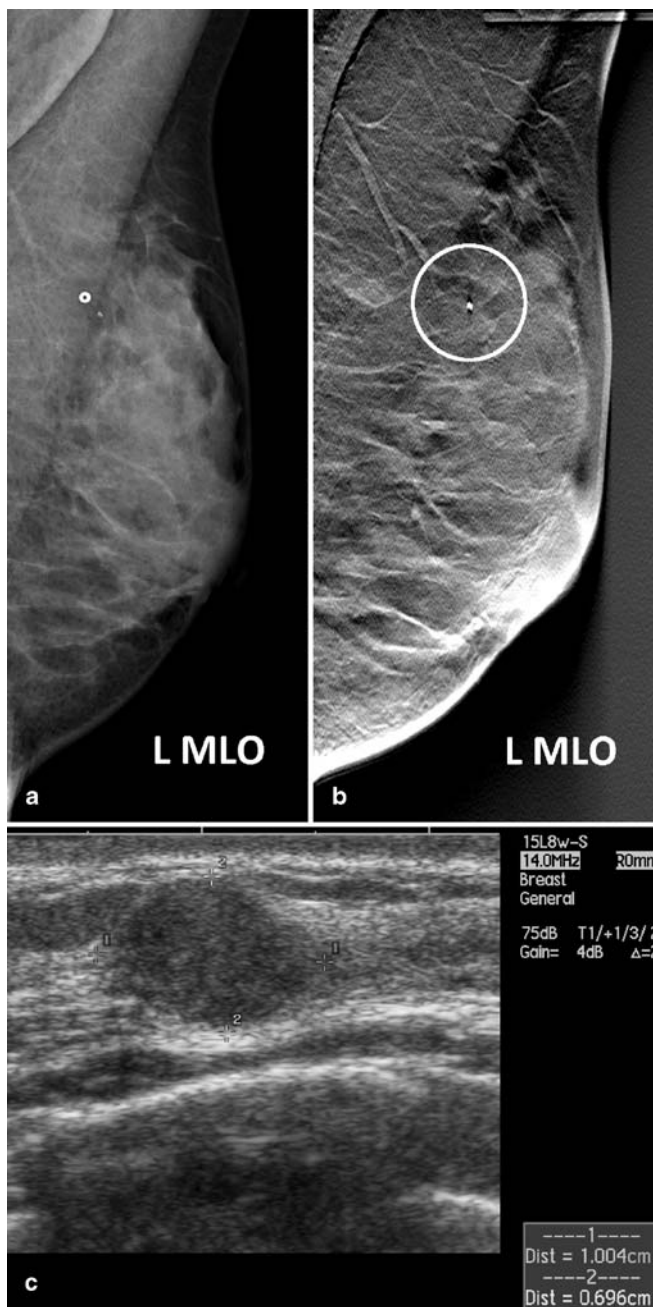


Fig. 3 Patient with a palpable 10-mm, grade 3, invasive ductal carcinoma not clearly visualized on BT or DM images, but seen on US. **(a)** MLO DM view shows normal, dense tissue and non-specific scattered calcifications. There is a marker over a palpable mass in the upper outer quadrant. **(b)** MLO BT view shows normal dense tissue and benign-appearing calcifications, but no mass in the area of the palpable mass (circle). **(c)** The US image over the palpable finding shows a hypoechoic oval mass not seen on either DM or BT images

The sensitivity of mammography is suboptimal in dense breasts [2–4]. As suggested by the present study, a small cancer can be concealed even by a moderate amount of dense tissue (Fig. 2). In the current study, the DM view in

Table 3 Visibility of 40 breast cancers in two-view digital mammography (DM) and one-view breast tomosynthesis (BT)

Two-view DM	One-view BT	N
Not visible	Not visible	4
Not visible	Questionably visible	1
Not visible	Visible	2 ^a
Questionably visible	Visible/clearly visible	8 ^b
Visible/clearly visible	Visible/clearly visible	24
Clearly visible	Not visible/not included	1
Total		40

^a“Not visible” category in Table 1 previously contained four one-view-only cancers now displayed on the second view here

^bSeven cancers became more visible on two-view mammogram when compared to one-view mammogram

which the lesion was most difficult to recognize was chosen for BT. If the lesion was equally well seen in both views on DM, the mediolateral oblique (MLO) view was chosen for BT. Actually, the MLO view was chosen in all but three cases. Thus, the cancers were considered more obvious in the craniocaudal (CC) view in the majority of cases. This may be explained by the common distribution of the fibroglandular tissue, which in the CC view is located in the subareolar region and in the upper outer quadrant. The fibroglandular tissue in the MLO view tends to overlap with most of the breast. Thus, even the superimposition of a moderate amount of fibroglandular tissue seems to hamper the detection of a small tumour in the MLO view. This is an observation that was made 30 years ago as part of an analysis of the number of views to be used in screening with mammography for breast cancer [30]. Thus, two-view DM is superior to one-view for cancer detection, as the distribution of fibroglandular

Table 4 Suspicion for malignancy by BIRADS classification of 40 breast cancers in one-view digital mammography (DM) and one-view breast tomosynthesis (BT)

One-view DM BIRADS	One-view BT BIRADS	N
1	1	4
2	2	1
1, 2	3, 4, 5	11
3	3	1
3	4, 5	10
4	1 ^a	1
4	4	9
4	5	3
Total		40

^aSpiculated mass in axillary tail not included in tomosynthesis field of view

Table 5 Suspicion for malignancy by BIRADS classification of 40 breast cancers in two-view digital mammography (DM) and one-view breast tomosynthesis (BT)

Two-view DM BIRADS	One-view BT BIRADS	N
1	1	5
1, 2	3, 4, 5	4
2	2	1
3	3	1
3	4, 5	8
4	4	17
4	5	3
5	5	1
Total		40

tissue is different in both. In BT, the distribution of fibroglandular tissue is not as much a concern, as the problem of superimposition is reduced in a tomographic technique.

The problem of obscuring superimposed tissue may be further compounded by the morphology of the lesion. Specifically, less characteristic or round tumour morphology may be more adversely affected by superimposition than the typically spiculated tumour. Two tumours detected with BT but unsuspected with DM were spiculated. Of the five cases not seen on MLO BT, four were also not seen on the 2D CC view. A rounded or non-specific growth pattern and the fact that the cancers were embedded in the dense tissue may have been the main factors explaining the nonvisibility of these lesions.

We also observed cancers characterized by pleomorphic calcifications, which contained DCIS as well as large

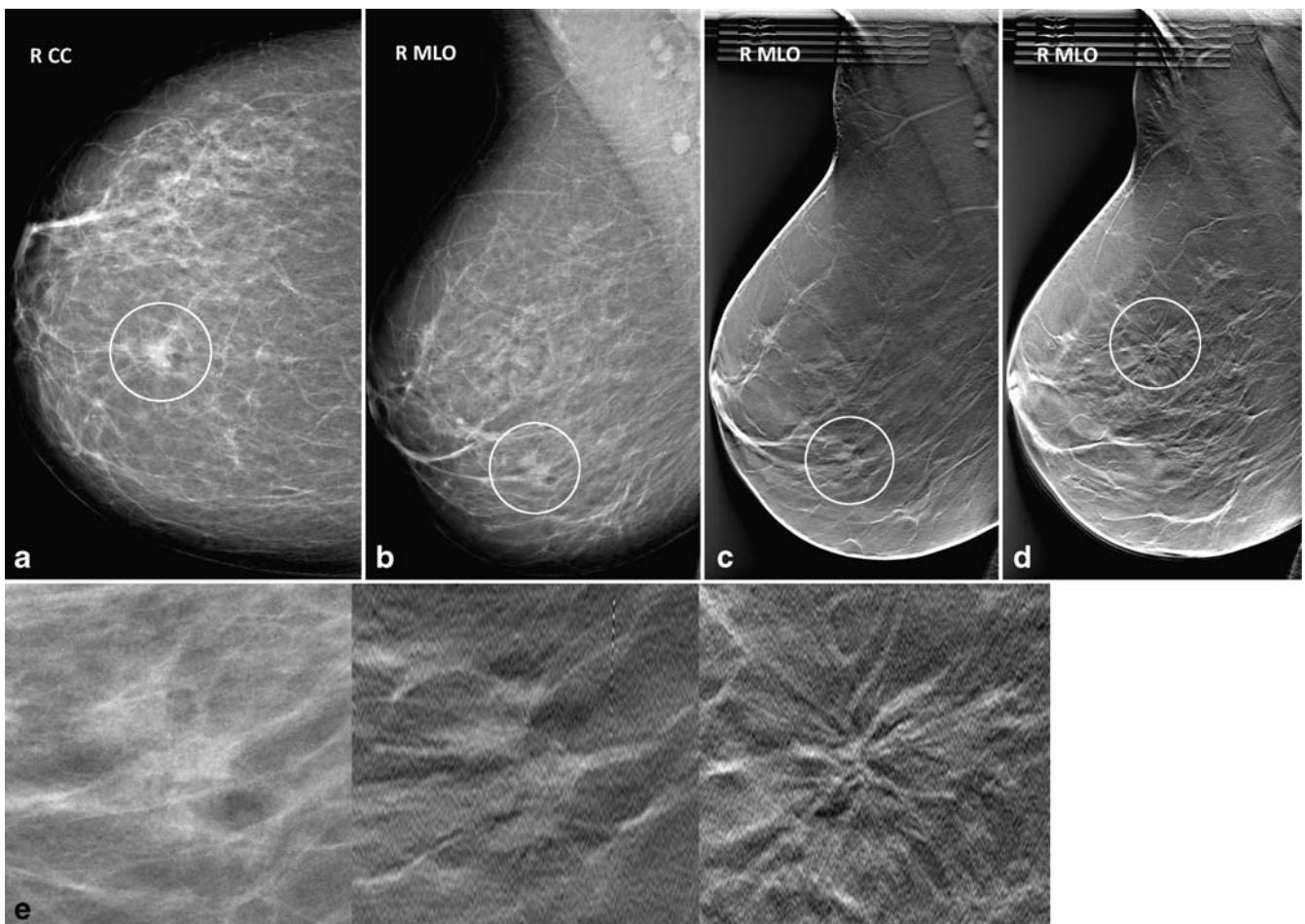


Fig. 4 Patient with multifocal carcinoma. (a) DM CC view image shows a medially located spiculated mass (circle). (b) DM MLO view image shows the same mass in the lower right breast (circle). (c) BT MLO of the same breast reveals the mass from (A) and (B) on slice 33 representing a 17-mm invasive lobular carcinoma grade 1. (d)

Another BT MLO slice (slice 20) reveals a second spiculated mass in the upper breast that is not visible in either DM view-(A) or (B)-or on the US exam. This was a 9-mm invasive lobular carcinoma. (e) Left to right: magnified views of the outlined regions in Fig. 4 B to D

components of IDC. Although the DCIS calcified portion was seen, the noncalcified large invasive component was not possible to identify due to lack of edge characteristics or attenuation differences. We hypothesize that the invasive component of these tumours had a non-specific growth pattern and blended with the surrounding tissues. However, it should be noted that calcifications were as detectable in BT images as in DM images in this patient series. The distribution of the calcifications was well demonstrated, but the morphologic details of the individual calcification were not as well visualized on BT.

A limitation of the present study was that it involved a non-blinded review. For a more accurate description of

sensitivity, a larger series of cases, including normal cases, should be included with independent reading of DM and BT images. Despite this limitation, the results of this study are relevant, as it to our knowledge included the largest breast cancer series imaged with BT and published to date. For this series, the results indicated that single-view BT ultimately may have a higher sensitivity for breast cancer detection than either single- or two-view DM.

Acknowledgments The study was supported by the Swedish Cancer Society, the European Union 5th Framework Program, the Cancer Foundation of Malmö University Hospital, and by the Sydney L. Frank Foundation

References

- Warren Burhenne LJ, Wood SA, D'Orsi CJ et al (2000) Potential contribution of computer-aided detection to the sensitivity of screening mammography. *Radiology* 215:554–562
- Kerlikowske K, Grady D, Barclay J, Sickles EA, Ernster V (1996) Effect of age, breast density, and family history on the sensitivity of first screening mammography. *JAMA* 276:33–38
- Carney PA, Miglioretti DL, Yankaskas BC et al (2003) Individual and combined effects of age, breast density, and hormone replacement therapy use on the accuracy of screening mammography. *Ann Intern Med* 138:168–175
- Kolb TM, Lichy J, Newhouse JH (2002) Comparison of the performance of screening mammography, physical examination, and breast US and evaluation of factors that influence them: an analysis of 27,825 patient evaluations. *Radiology* 225:165–175
- Ikeda DM, Andersson I, Wattsgård C, Janzon L, Linell F (1992) Interval carcinomas in the Malmö Mammographic Screening Trial: radiographic appearance and prognostic considerations. *AJR Am J Roentgenol* 159:287–294
- Birdwell RL, Ikeda DM, O'Shaughnessy KF, Sickles EA et al (2001) Mammographic characteristics of 115 missed cancers later detected with screening mammography and the potential utility of computer-aided detection. *Radiology* 219:192–202
- Bochud FO, Valley JF, Verdun FR, Hessler C, Schnyder P (1999) Estimation of the noisy component of anatomical backgrounds. *Med Phys* 26:1365–1370
- Burgess AE, Jacobson FL, Judy PF (2001) Human observer detection experiments with mammograms and power-law noise. *Med Phys* 28:419–437
- Ruschin M, Timberg P, Båth M et al (2007) Dose dependence of mass and microcalcification detection in digital mammography: free response human observer studies. *Med Phys* 34:400–407
- Hilleren DJ, Andersson IT, Lindholm K, Linell FS (1991) Invasive lobular carcinoma: mammographic findings in a 10-year experience. *Radiology* 178:25–26
- Lewin JM, Hendrick RE, D'Orsi CJ et al (2001) Comparison of full-field digital mammography with screen-film mammography for cancer detection: Results of 4,945 paired examinations. *Radiology* 218:873–880
- Skaane P, Skjennald A (2004) Screen-film mammography versus full-field digital mammography with soft-copy reading: randomized trial in a population-based screening program—the Oslo II study. *Radiology* 232:197–204
- Pisano ED, Gatsonis C, Hendrick E et al (2005) Diagnostic performance of digital versus film mammography for breast-cancer screening. *N Engl J Med* 353:1773–1783
- Skaane P, Hofvind S, Skjennald A (2007) Randomized trial of screen-film versus full-field digital mammography with soft-copy reading in population-based screening program: Follow-up and final results of Oslo II study. *Radiology* 244:708–717
- Niklason LT, Christian BT, Niklason LE et al (1997) Digital tomosynthesis in breast imaging. *Radiology* 205:399–406
- Wu T, Stewart A, Stanton M et al (2003) Tomographic mammography using a limited number of low-dose cone-beam projection images. *Med Phys* 30:365–380
- LO JY, Baker JA, Orman J, Mertelmeier T (2006) Breast tomosynthesis: Initial clinical experience with 100 human subjects (abs). In: Radiological Society of North America scientific assembly and annual meeting program. Oak Brook, Ill: Radiological Society of North America SSG01-03, p 335
- Rafferty EA (2003) Breast tomosynthesis. *Adv Digital Radiography: RSNA Categorical Course in Diagnostic Radiology Physics*, pp 219–226
- Varjonen M (2006) Three-dimensional (3D) digital breast tomosynthesis (DBT) in the early diagnosis and detection of breast cancer. Thesis, Tampere University of Technology, Tampere, Finland
- Good WF, Abrams GS, Catullo VJ, Chough DM, Ganott MA, Hakim CM, Gur D (2008) Digital breast tomosynthesis: A pilot observer study. *AJR* 190:865–869
- Poplack SP, Tosteson TD, Kogel CA, Nagy HM (2007) Digital breast tomosynthesis: initial experience in 98 women with abnormal digital screening mammography. *AJR Am J Roentgenol* 189:616–623

-
22. Moore RH, Kopans DB, Rafferty EA et al (2007) Initial callback rates for conventional and digital breast tomosynthesis mammography comparison in the screening setting. (Abs). In: Radiological Society of North America scientific assembly and annual meeting program. Oak Brook, Ill: Radiological Society of North America SSG01-01, p 381
 23. Bissonnette M, Hansroul M, Masson E et al (2005) Digital breast tomosynthesis using an amorphous selenium flat panel detector. *Proc SPIE* 5745:529–540
 24. Zoetelief J, Fitzgerald M, Leitz W, Säbel M (1996) European protocol on dosimetry in mammography. Publication EUR 16263 EN, Brussels, Belgium: European Commission
 25. Mertelmeier T, Orman J, Haerer W, Dudam MK (2006) Optimizing filtered backprojection reconstruction for a breast tomosynthesis device. *Proc SPIE* 6142:131–142
 26. Orman J, Mertelmeier T, Haerer W (2006) Adaptation of image quality using various filter setups in the filtered backprojection approach for digital breast tomosynthesis. In: Astley SM, Brady M, Rose C, Zwigelaar R (eds) *Proceedings of the 8th international workshop on digital mammography*. IWDM, Manchester, UK: Springer, Berlin, pp 175–182
 27. “NEMA Standards Publications PS 3.14 (1998) Digital Imaging and Communications in Medicine (DICOM), Part 14: Grayscale Standard Display Function.” National Electrical Manufacturers Association, 2101 L Street, N.W., Washington, D.C., 20037
 28. Båth M, Månsson LG (2007) Visual grading characteristics (VGC) analysis: a non-parametric rank-invariant statistical method for image quality evaluation. *Br J Radiol* 80:169–176
 29. Metz CE. The computer program ROCKIT 0.9B. Available from C. Metz, Dept of Radiology, University of Chicago, Chicago, IL, USA, <http://www-radiology.uchicago.edu/krl/>
 30. Andersson I, Hildell J, Muhlow A, Pettersson H (1978) Number of projections in mammography: influence on detection of breast disease. *AJR Am J Roentgenol* 130:349–351